

RESEARCH DIVISION

1100 SOUTH 34TH AVENUE, MINNEAPOLIS, MINNESOTA 55440-1612-053-8100

**CONTROL DATA**  
CORPORATION

CR-135176

VARIABILITY AND TRANSPORT OF OZONE  
AT THE TROPOPAUSE FROM THE  
FIRST YEAR OF GASP DATA

By

G. D. Nastrom

Research Report No. 4

February 22, 1977

Contract NAS 2-7807

For

NASA-Lewis Research Center  
Cleveland, OH 44135

Distribution of this report is provided in the interest of information exchange. Responsibility for the contents resides in the authors or organization that prepared it.

1. Report No. NASA CR-135176		2. Government Accession No.		3. Recipient's Catalog No.	
4. Title and Subtitle VARIABILITY AND TRANSPORT OF OZONE AT THE TROPOPAUSE FROM THE FIRST YEAR OF GASP DATA				5. Report Date FEBRUARY 1977	
				6. Performing Organization Code	
7. Author(s) G. D. NASTROM				8. Performing Organization Report No. RESEARCH REPORT NO.4	
9. Performing Organization Name and Address RESEARCH DIVISION CONTROL DATA CORPORATION 8100 SOUTH 34th STREET MINNEAPOLIS, MN 55440				10. Work Unit No.	
				11. Contract or Grant No. NAS 2-7807	
12. Sponsoring Agency Name and Address NATIONAL AERONAUTICS AND SPACE ADMINISTRATION WASHINGTON, DC 20546				13. Type of Report and Period Covered CONTRACTOR REPORT	
				14. Sponsoring Agency Code	
15. Supplementary Notes PROJECT MANAGER - JAMES D. HOLDEMAN, AIRBREATHING ENGINES DIVISION, NASA LEWIS RESEARCH CENTER, CLEVELAND, OHIO 44135					
16. Abstract  Ozone measurements taken from commercial airliners (GASP data) have monthly mean patterns very similar to ozonesonde results. A significant variation in the east-west spatial autocorrelation function of ozone near the tropopause has a length of about 1900 km. The relationships of ozone near the tropopause with potential vorticity, temperature, and distance from the tropopause are examined. GASP data are also used to estimate the vertical and horizontal fluxes of ozone near the tropopause. The annual average flux of ozone into the troposphere at 30-50°N is $7.8 \times 10^{10}$ molecules $\text{cm}^{-2} \text{ s}^{-1}$ , which is nearly the same as indirect estimates based on surface ozone data, thus supporting the hypothesis that the amount of ozone in the troposphere is essentially controlled by injection from the stratosphere. The present GASP estimates of the total flux of ozone into the troposphere verify the model results of Cunnold, et al (1975), although the distribution of flux between mean motions and diffusion is different and thus suggests that models with coarse horizontal resolution must continue to parameterize much vertical transport by diffusion coefficients. Monthly estimates of the horizontal transient eddy flux of ozone are generally smaller than seasonal or yearly results based on ozonesonde data. This is perhaps because the present estimates are made over monthly periods to reduce the influence of correlation between the annual variations in ozone and meridional wind. The available data support the hypothesis that transient eddy fluxes of ozone have large longitudinal variations.					
17. Key Words (Suggested by Author(s)) Ozone Tropopause Variability Vertical Flux Horizontal Flux			18. Distribution Statement  UNCLASSIFIED - UNLIMITED		
19. Security Classif. (of this report) UNCLASSIFIED		20. Security Classif. (of this page) UNCLASSIFIED		21. No. of Pages	
				22. Price*	

\* For sale by the National Technical Information Service, Springfield, Virginia 22161

TABLE OF CONTENTS

	Page
I. INTRODUCTION . . . . .	1
II. DATA . . . . .	1
III. RESULTS. . . . .	3
A. Variability of Ozone . . . . .	3
1. Small-Scale Variability Near the Tropopause. . . . .	3
2. Mean Ozone Amounts . . . . .	5
B. Relationship of Ozone to Other Variables . . . . .	6
C. Flux of Ozone. . . . .	7
1. Vertical Ozone Flux. . . . .	7
2. Horizontal Ozone Flux. . . . .	11
IV. CONCLUSIONS AND RECOMMENDATIONS. . . . .	13
REFERENCES . . . . .	15
TABLES 1-5 . . . . .	
FIGURES 1-11 . . . . .	

LIST OF FIGURES

- Figure 1. Heavy line is monthly mean variation of GASP ozone at 11-12 km, 36-42°N from March, 1975, through March, 1976. A 1-2-1 smoothing has been applied. Dotted lines are ozonesonde means at 40°N from Wilcox, et al (1975). Units:  $10^{11}$  molecules  $\text{cm}^{-3}$ .
- Figure 2. Distance lagged autocorrelation coefficients of ozone along east-west flight legs, based on 33 flights. See text.
- Figure 3. Distance lagged autocorrelation coefficients of ozone along east-west flight legs, for all data and by season. The dotted line on each chart is the least squares fit of  $R(L) = \exp(VL)$  to the "average" data and the solid lines are the fits to the seasonal data. N is the number of flights and d is the integral space scale of R(L). See text.
- Figure 4. Monthly "zonal" means of ozone (ppbv) at 11-12 km. The dotted lines show the latitudes of the monthly mean tropopause at 11.5 km. Note that the Flattery tropopause model was used until December, 1975, and the Gustafson model thereafter.
- Figure 5. Solid lines are "zonal" means of ozone (ppbv) of  $10^\circ$  latitude belts for combined March data (1975 and 1976). The dashed line is mean tropopause location, and the dotted lines are "zonal" means of potential vorticity ( $10^{-6}$  deg  $\text{hPa}^{-1} \text{ s}^{-1}$ ), for each belt.
- Figure 6. Correlation coefficients of ozone with temperature for combined March data (1975 and 1976). The dotted line is mean tropopause location.
- Figure 7. Correlation coefficients of ozone with temperature at 11-12 km by month. The dotted lines show the latitudes of the monthly mean tropopause at 11.5 km.
- Figure 8. Correlation coefficients of ozone with potential vorticity for combined March data (1975 and 1976). The dotted line is mean tropopause location.
- Figure 9. Correlation coefficients of ozone with potential vorticity at 11-12 km by month. The dotted lines show the latitudes of the monthly mean tropopause at 11.5 km.
- Figure 10. Northward flux of ozone by transient eddies at 11-12 km by month (units:  $10^{-9} \text{ g cm}^{-2} \text{ s}^{-1}$ ). The dotted lines show the latitudes of the monthly mean tropopause at 11.5 km. To avoid confusion, isoline labels are underlined.

LIST OF FIGURES (CONT'D)

Figure 11. Northward flux of ozone by transient eddies for combined March data (1975 and 1976). Units:  $10^{-9} \text{ g cm}^{-2} \text{ s}^{-1}$ . The dotted line is mean tropopause location, and isoline labels have been underlined to avoid confusion.

## I. INTRODUCTION

This report summarizes the results of an analysis of the first year of Global Atmospheric Sampling Program (GASP) data. GASP is an ongoing effort to measure ozone and other trace constituents with instruments placed on commercial airliners. Details on instrumentation, routes, etc., can be found elsewhere (Holdeman, et al, 1976, and references therein). A case study of one series of flights, including examples of the data obtained has been made by Falconer and Holdeman (1976). Although the present data span only thirteen months, they should serve to establish the basic seasonal patterns.

## II. DATA

All ozone data used here are from the GASP measurements archived on tapes VL001-VL004 (Holdeman, et al, 1976). A monthly summary of the amount of data and the limits of its geographical distribution is in Table 1, and examples of the number of observations are in Table 2. Although there were a few flights around the world or into the Southern Hemisphere, the bulk of the flights were within the contiguous United States, from the mainland to Hawaii, and from the United States to Europe. The in situ ozone mixing ratio, measured by an ultraviolet absorption photometer, is reported every five minutes (i.e., about every 75 km), but about three observations per hour are missed because the instrument is in a calibration mode. Although data are taken at all flight altitudes above 6 km, most observations are taken between 10 and 12 km altitude. Flight level pressure, temperature, wind velocity, and an indicator from the aircraft accelerometer of turbulence occurrence are reported with each ozone observation. Whenever the accelerometer reading exceeds a critical value, ozone amount is given every five seconds

for the next 60 seconds; but in these cases the data were averaged over one minute intervals and each average was counted as only one observation.

Supplementary parameters were computed for each ozone observation from the NMC Northern Hemisphere grids of isobaric height fields and tropopause pressure fields, which are available at 00 and 12 GMT. The map time nearest the mid-time of each flight was used to compute aircraft altitude, tropopause separation pressure ( $P_{\text{Trop}} - P_{\text{Aircraft}}$ ), geostrophic winds and vorticity, potential vorticity, and the algebraic sign of the vertical velocity from the diagnostic omega equation (definitions and discussion of the latter four parameters are given in most texts, e.g., Holton (1972) on pages 36, 66, 69, and 112, respectively). Linear interpolation between NMC grid points along isobaric surfaces and with height was used to estimate the needed parameters at the aircraft's location for each ozone observation. An exception is that the lapse of potential temperature used in computing the potential vorticity was determined from the three pressure surfaces centered nearest the flight level pressure. All derivatives were estimated by finite differences.

In an effort to establish confidence in the GASP data, mean ozone values from GASP are compared with those from North American ozonesondes (from Wilcox, et al, 1975) in Figure 1. As most of the GASP data at 40-50°N were taken over North America, differences due to longitude should be small. March data from 1975 and 1976 have been averaged although individual values are also shown. Linear interpolation was used for November's absent data, and a 1-2-1 smoothing has been applied. The GASP data appear to provide mean values comparable to those from ozonesondes, as the small seeming discrepancies found in Figure 1 will likely be resolved with more data.

### III. RESULTS

#### A. VARIABILITY OF OZONE

1. Small-Scale Variability Near the Tropopause. Before discussing the large-scale variability of ozone, it is interesting to examine the spatial autocorrelation of ozone along individual flight legs. A total of 33 flight legs was found which are at constant pressure level throughout, at least 1200 km long, oriented nearly east-west, at least half the data at 5-minute intervals, turbulence free, and do not intersect the tropopause. The lagged autocorrelation coefficients were computed over each flight leg, and the average of the 33 values is given in Figure 2. The vertical lines in the figure extend one standard error of the mean above and below the mean at selected lags. The curve in Figure 2 can be crudely approximated as the product of an exponential decay (i.e., red-noise persistence) and a cosine variation with half-wavelength near 950 km (wavelength near 1900 km). Note that red-noise persistence is characteristic of all atmospheric variables, and that 1900 km is about the distance across intense troughs or ridges. A three-point parabolic curve-fit of the power spectrum of the data in Figure 2 places the peak power at 2150 km wavelength.

Variations with latitude, season, or altitude showed significant differences only between late summer and late winter. The first portion of each autocorrelation function is given in Figure 3, and the least squares fit of  $R(L) = \exp(VL)$ , where  $L$  is the lag and  $V$  is the slope in natural logarithmic coordinates, appears as a straight, solid line on each chart. The corresponding least squares fit of the autocorrelation function over all 33 flights is shown by the dotted lines for comparison. The autocorrelation function falls off less rapidly in winter than in summer, perhaps reflecting



the greater organization of atmospheric motion patterns in winter. Parallel seasonal behavior of the autocorrelation function of wind has been found by Buell (1972).

A characteristic scale of ozone variability can be estimated by

$$d = \int_0^{\infty} R(L) dL$$

The resulting values of  $d$  for each season, based on  $R(L) = \exp(-VL)$ , are given in Figure 3. The east-west distance between independent observations taken at the same pressure level is thus  $2d$  (Leith, 1973). These estimates may be useful to others using ozone data collected at constant pressure levels, or as a lower bound for the independence of total ozone data. They should not be used to estimate the number of independent observations of the present GASP data set because the criteria employed to select the 33 flight legs used here are not fulfilled on most flights. Especially important is that many flight legs are not east-west, and the correlation function of ozone is expected to be non-isotropic (as the correlation function of wind is; Buell, 1972). It is planned to compute the north-south autocorrelation function after suitable data have been collected, but it was not possible with the present sample.

The results given in Figure 2 may be of interest to those analyzing other types of ozone data. It is well-known from sampling theory that measurements should be taken at twice the highest frequency of variability to be resolved. Thus, measurements of ozone near the tropopause should be spaced no more than 950 km in the east-west direction or significant aliasing will occur. Because total ozone is highly correlated with the height of the

100 hPa surface, it probably has a similar scale of preferred variability. In that case, widely spaced data (e.g., the Nimbus IV orbits which are about 2000 km apart at  $45^{\circ}\text{N}$ ) may be useful only for making zonal or monthly means because synoptic analyses may be severely aliased. There do not seem to have been any studies on this problem.

2. Mean Ozone Amounts. The average ozone amount by month between 11 and 12 km is shown in Figure 4, where data in each latitude zone have been averaged regardless of longitude, as in a zonal mean. The intersection of the NMC tropopause with the 11.5 km height surface is shown by the dotted lines. Note that NMC used the so-called Flattery method for locating the tropopause before December 15, 1975, and the Gustafson method thereafter. Preliminary comparisons (Holdeman, et al, 1976) indicate that the Gustafson method often appears to locate the tropopause at lower altitudes. Thus, the more southerly tropopause line in March, 1976, compared with 1975, may be an artifact of the NMC analysis scheme. Further discussion of the tropopause analysis schemes is beyond the scope of this report, and in the results presented here any possible differences were neglected unless stated otherwise. In Figure 4, the ozone isopleths are nearly parallel with the tropopause line, especially near the tropopause line, with largest ozone values in the stratosphere. A corresponding relation with the tropopause is found on the height-latitude section of average ozone in March, 1975 and 1976 (Figure 5). Also evident in Figures 4 and 5 is the small variability of mean tropospheric ozone, except near the tropopause, with latitude as well as height, suggesting that ozone in the upper troposphere is well mixed. The large variations of ozone nearest the tropopause are probably associated with stratospheric-tropospheric exchange, discussed in detail later.

## B. RELATIONSHIP OF OZONE TO OTHER VARIABLES

The variations in ozone amount at a given location are closely related to the variations in many other atmospheric parameters. The relationships discussed here are those with distance from the tropopause, potential vorticity, and temperature, although other parameters could also have been used. The first two parameters were selected because they are coupled with ozone transport while temperature was selected primarily because it historically has been used.

In Figures 4 and 5, it was seen that mean ozone amount is related to the tropopause location. This relationship is shown further by the data in Table 3, where observations are stratified both by height and by tropopause separation pressure ( $P_{\text{Trop}} - P_{\text{Aircraft}}$ ). Several points can be noted: (1) the mean ozone may decrease or increase with height in Table 3a, but always increases with increasing positive pressure difference in Table 3b; (2) the average variance about the level mean values in Table 3b is reduced about 40%, 60%, and 5% in March 1975, 1976, and October, respectively, compared with Table 3a; (3) the frequency distributions of ozone mixing ratios in March are often multi-modal in Table 3a, but not in Table 3b. The modal differences for the 0 to 50 hPa layer between March 1975 and March 1976 may be a consequence of the NMC tropopause models used, although there may be other explanations. Finally, (4) there is a close correspondence in Table 3a between the number of observations below the tropopause at each level and the frequency of occurrence of  $<100\text{ppbv}$ .

The correlation of ozone with temperature as a function of height and latitude during March is given in Figure 6. Large positive correlations are

found in the stratosphere while the correlations are generally negative and small in the troposphere, reflecting the change in sign in the vertical gradient of temperature at the tropopause. (It is expected that the tropopause line near  $35^{\circ}\text{N}$  would more nearly parallel the isolines if the Flattery tropopause model had been used in 1976.) Largest magnitudes are in the stratosphere in Figure 6 because in the stratosphere both ozone and temperature have large vertical gradients, while in the upper troposphere the vertical gradient of ozone is small. The zero correlation line occurs slightly below, rather than at, the NMC tropopause at mid-latitudes, presumably because near the tropopause descending air, which contains high ozone, is adiabatically warmed. Thus, sufficiently far from the tropopause the correlations arise primarily from the mean vertical structure of temperature and ozone, while near the tropopause the correlations arise from eddy activity. These results compare fairly well with those from ozonesondes (Dütsch, et al, 1970), although close comparison is not warranted because sonde data always refer to a particular level while the present results are for 1 km height intervals. Thus, interpretation in terms of vertical gradients does not apply to sonde results.

A similar pattern is found in Figure 7 where correlation coefficients of temperature and ozone at 11-12 km are given by month. The annual cycle in tropopause height induces an annual cycle in the correlation coefficients at 11-12 km in mid-latitudes.

The relationship between ozone and potential vorticity has been studied by Hering (1966) and Danielson (1968), among others. In adiabatic, frictionless flow, potential vorticity is conserved by an air parcel, just as ozone

would be if it were chemically inert. Monthly mean values of ozone and potential vorticity are compared in Figure 5. The close correspondence of the two fields (correlation coefficient=0.95) is similar to that found by Hering, but the present results show much more detail. In particular, note the apparent intrusions of ozone and potential vorticity below the tropopause near  $40^{\circ}\text{N}$ .

In the stratosphere, the small-scale variations of ozone also correlate well with potential vorticity variations as shown in Figures 8 and 9. The large annual cycle of the correlation coefficients (Figure 9) at 11-12 km at  $45^{\circ}\text{N}$  is induced by the annual cycle in tropopause height. An unexpected feature in Figure 9 is a small semiannual variation near  $25^{\circ}\text{N}$ , which may merit study if verified by further data.

### C. FLUX OF OZONE

1. Vertical Ozone Flux. In an effort to estimate stratospheric-tropospheric exchange from the present data, all ozone observations taken within 50 hPa of the tropopause and north of  $30^{\circ}\text{N}$  were sorted according to the sign of the associated vertical motion. The mean ozone in each motion group is given in Table 4, where it will be noted that the ozone associated with downward motion is always greater than that associated with upward motion. Assuming no net mass transfer across the tropopause, this implies there is a net downward flux of ozone, but to estimate the magnitude of the flux the mean magnitude of the vertical velocity at the tropopause is needed.

Case studies of the vertical velocity field suggest that near the tropopause its mean magnitude is a few tenths of a centimeter per second (Palmén and Newton, 1969), but detailed statistics for the Northern Hemisphere

do not appear to be available. In the statistical study by Angell (1975), based on Southern Hemisphere EOLE data, the cumulative frequency distribution 50% line is at  $0.5 \text{ cm s}^{-1}$ . Angell's results show a small variation with season, but that is neglected here as his model is probably valid only for guidance, e.g., it assumes a constant temperature lapse rate. The net flux of ozone across the tropopause, based on  $\overline{w} = 0.5 \text{ cm s}^{-1}$ , is given in Table 4. The estimates of uncertainty in Table 4 are the root-sum-square of the standard errors of the mean of the two motion groups for each season. The average yearly value,  $7.8 \times 10^{10} \text{ molecules cm}^{-2} \text{ s}^{-1}$ , compares well with the results of Fabian and Pruchniewicz (1976) who, using surface ozone data, estimate the flux to be 7.9 and 8.6 units at  $35^\circ$  and  $45^\circ\text{N}$ , respectively. This very close agreement supports the hypothesis that the amount of ozone in the troposphere is essentially controlled by injection from the stratosphere.

The use of the layer Trop  $\pm$  50 hPa is admittedly arbitrary, but not critical. When the layers Trop to Trop-100 or Trop to Trop+100 are used, the average yearly flux estimates are 9.2 and 7.4 units, respectively. It is interesting that the vertical flux is larger above the tropopause than below it. While the present results are too uncertain to draw any conclusions regarding possible vertical flux divergence, additional years of data may support computations of vertical flux divergence.

The vertical ozone transport estimates presented in Table 4 reflect only the transport by motions whose wavelength is longer than about 700 km, i.e., twice the spacing of the NMC grid at mid-latitudes. The transport of ozone by disturbances smaller than about 700 km can be estimated by assuming the

flux is the product of an eddy diffusion coefficient and the gradient of ozone across the tropopause. The diffusion coefficient at the tropopause used by Cunnold, et al (1975),  $3 \times 10^3 \text{ cm}^2 \text{ s}^{-1}$ , is adopted here, and the gradient of ozone is estimated by finite differences of mean values of layers 50 hPa thick and centered 25 hPa above and below the tropopause. The resulting estimates of the diffusive flux (Table 4) are only about 3% as large as the corresponding fluxes by large-scale motions. The diffusive flux in winter is based on layer mean values centered 75 and 25 hPa above the tropopause for two reasons. The vertical gradient of ozone changes rapidly near the tropopause. Also, the NMC tropopause model used after December 15, 1975, apparently yields consistently high estimates of the tropopause pressure (Holdeman, et al, 1976).

It is interesting to compare the present estimates of ozone transport across the tropopause with the model results of Cunnold, et al (1975), keeping in mind that the latitude band  $30\text{-}50^\circ\text{N}$  may only poorly represent global mean values and that the results in Table 4 do not include transport by zonal mean motions. Using 10 km as the mean global tropopause height, the transport by large scale eddies is  $31.4 \text{ metric tons s}^{-1}$ , and that by diffusion is  $0.7 \text{ ton s}^{-1}$ . Cunnold, et al (1975), give corresponding values of 27 and 5  $\text{tons s}^{-1}$ , respectively. Thus, although the total flux is the same (perhaps fortuitously) it is distributed differently. This may be due to their model's truncation at zonal wavenumber 6, for significant ozone variations near the tropopause are associated with wavelengths near 1900 km (wavenumber 16 at  $40^\circ\text{N}$ ), as shown in Figure 2. This suggests that if dynamical models are truncated at a low wavenumber, the proper flux of ozone into the tropospheric sink must be accommodated by parameterized diffusion.

The preceding results are apparently the first direct estimates of ozone flux across the tropopause. The detailed mechanism whereby this flux occurs has been shown to be tropopause folding (Danielson, 1968). The folds, or ruptures, of the tropopause are mesoscale phenomena which are not retained on most global-scale analyses, so their effect has been parameterized by a cyclone index (Reiter, 1975) in the past. However, as Cunnold, et al (1975), point out, knowledge of the detailed transfer mechanism is not necessary for global models if the downward transport of ozone is associated with large-scale motions. The close agreement of the present estimates with those of Fabian and Pruchniewicz (1976), from surface ozone data, supports the latter hypothesis because the NMC grid can resolve only large-scale systems and is too coarse to resolve folds in the tropopause.

2. Horizontal Ozone Flux. Estimates of the ozone flux by transient eddies are given in Figures 10 and 11. Largest fluxes are generally found in the stratosphere during late winter although negative values occurred in March - May, 1975, at mid-latitudes. The latter fact is contrary to expectations, as studies of the transient eddy flux based on ozonesonde data (e.g., Hering, 1966; Hutchings and Farkas, 1971) have found positive fluxes throughout the lower stratosphere. This seeming discrepancy may be related to sampling deficiencies or 1975 may have been a very unusual year. A further explanation is the differing length of period over which the transients are computed. Hering combined all data over half-year periods, and Hutchings and Farkas combined all data regardless of season, while in the present study monthly periods have been used. The correlation of the annual cycles in ozone and meridional wind thus contributes very little to the present monthly flux estimates. To illustrate the effect of using differing time periods



for defining "transient" motions, imagine the meridional wind and the ozone amount to change from month to month, but to have a constant value within each month. If one then computes transient eddy fluxes over monthly intervals, the results would be zero, but if periods longer than a month were used to compute fluxes, large results would be obtained. The annual cycle in meridional wind at a given location arises primarily from the growth and collapse of standing spatial waves. Standing waves induce a flux of ozone only if ozone also has a standing wave pattern, but the magnitude, or even the algebraic sign, of the standing eddy flux cannot be determined from single station data. Because the annual cycles in ozone and meridional wind at one location are not truly transients in the desired sense, they should be removed before computing transient eddy fluxes.

Indeed, the "transient" eddy flux at 11-12 km at 40-50°N based on all GASP data from December - May is  $49.5 \times 10^{-9} \text{ g cm}^{-2} \text{ s}^{-1}$ , and in June - October it is 2.3 units, in good agreement with Hering's values (40 and 8 units, respectively), while the averages of the monthly fluxes are 9.3 and 5.3 units, respectively. In computing the latter value, the July and November fluxes were estimated from Figure 10 to be 0 and 6 units, respectively. The difference between the seasonal (49.5, 2.3) and monthly average (9.3, 5.3) values is well accounted for by the correlation of the monthly means of ozone and meridional wind. When monthly means of ozone and meridional wind are used to compute seasonal fluxes, the values 42.3 and -1.6 units result. Clearly, the averages of the monthly fluxes (9.3, 5.3) are the most physically meaningful estimates.

Although the influence of seasonal variations is minimized in Figures 10 and 11, these results have noteworthy shortcomings. They may contain a contribution from possible standing eddy fluxes because all data have been used in this first effort, regardless of longitude. However, most data are taken from  $65^{\circ}$  -  $120^{\circ}$ W, so these results are not true zonal mean values, and there is no reason to expect zonal symmetry of transient eddy fluxes. In fact, because synoptic disturbances are known to have preferred tracks, distinct asymmetry of the transient eddy flux should be expected. This hypothesis is supported by the limited data during March in Table 5, where transient eddy fluxes at  $40^{\circ}$ - $50^{\circ}$ N are given for  $60^{\circ}$  longitude zones. As additional data become available, the zonal variations of eddy flux can be studied in more detail.

#### IV. CONCLUSIONS AND RECOMMENDATIONS

The first year of GASP ozone data has been summarized. The patterns of ozone variability given here are very similar to previous results based on ozonesondes. It is verified that ozone is well-correlated with distance from the tropopause (more so in spring than in autumn), temperature, and potential vorticity. A few other points seem warranted:

1. A significant scale of east-west ozone variability near the tropopause (about 1900 km) is very close to the synoptic disturbance scale. Detection of this feature from ground based or satellite data would be unlikely, but is possible from GASP data because it is homogeneous, local, and has high spatial observational frequency.

2. The current data are well suited for studying ozone transport across the tropopause as well as by transient eddies. The relatively large

volume of GASP data permit computing monthly fluxes, thus minimizing the contribution from correlations of the annual cycles.

3. It is suggested the transient eddy flux varies substantially with longitude.

4. If the GASP route structure is expanded to include the Soviet Union, it may be possible to also compute standing eddy fluxes of ozone near the tropopause.

5. Continued data collection will permit refining and expanding the present results. In particular, relatively large quantities of data from Australia and Southern Asia will soon be available, which may help better understand ozone transport by tropical circulation systems.

#### Acknowledgment

Helpful comments by Dr. A. D. Belmont are gratefully acknowledged.

## References

- Angell, J., 1975: The field of mean vertical velocity at 200 mb in south temperate latitudes as estimated from EOLE constant level balloon flights. Quart. J. R. Met. Soc., 101, 629-636.
- Buell, C., 1972: Correlation functions for wind and geopotential on isobaric surfaces. J. Appl. Meteor., 11, 51-59.
- Cunnold, D., F. Alyea, N. Phillips, and R. Prinn, 1975: A three-dimensional dynamical-chemical model of atmospheric ozone. J. Atmos. Sci., 32, 170-194.
- Danielson, E., 1968: Stratospheric-tropospheric exchange based on radioactivity, ozone, and potential vorticity. J. Atm. Sci., 25, 502-518.
- Dütsch, H., 1974: The ozone distribution in the atmosphere. Can. J. Chem., 52, 1491-1504.
- Dütsch, H., W. Züllig, Ch. Ling, 1970: Regular ozone observation at Thalwil, Switzerland and Boulder, Colorado. LAPETH-1, Zürich, 279pp.
- Fabian, P., and P. Pruchniewicz, 1976: Final Report on Project "Troposphärisches Ozon". Max-Planck Institut für Aeronomie, Lindau, 28pp.
- Falconer, P., and J. Holdeman, 1976: Measurements of atmospheric ozone made from a GASP-equipped 747 airliner: mid-March, 1975. Geophys. Res. Lett., 3, 101-104.
- Hering, W., 1966: Ozone and atmospheric transport processes, Tellus, 18, 329-336.

- Holdeman, J., F. Humenik, and E. Lezberg, 1976: NASA Global Atmospheric Sampling Program (GASP) data report for Tape VL0004. NASA TMX-73574, 47pp.
- Holton, J., 1972: Introduction to Dynamic Meteorology, Academic, New York, 319pp.
- Hutchings, J., and E. Farkas, 1971: The vertical distribution of atmospheric ozone over Christchurch, New Zealand, Quart. J. R. Met. Soc., 97, 249-254.
- Leith, C., 1973: The standard error of time-average estimates of climatic means, J. Appl. Meteor., 12, 1066-1069.
- Palmén, E., and C. Newton, 1969: Atmospheric Circulation Systems, Academic, New York, p.540.
- Reiter, E., 1975: Stratospheric-tropospheric exchange processes. Rev. Geophys. Spa. Phys., 13, 459-474.
- Wilcox, R., G. Nastrom, and A. Belmont, 1975: Periodic analysis of total ozone and its vertical distribution. NASA-CR-137737, 51pp. Available from NTIS, abstract no. N75-32657. A condensed, revised version of this material is in J. Appl. Meteor., March, 1977, under the same title.

Table 1. Summary of GASP data.

Month	Total Flights	Total Obs.	Latitude Range	Longitude Range
Mar 1975	57	1263	9N-61N	180E-180W
Apr	26	554	19N-47N	75W-159W
May	66	1625	23S-47N	45W-114E
Jun	35	908	19N-45N	84W-159W
Jul	3	78	21N-41N	84W-159W
Aug	16	434	21N-47N	84W-159W
Sep	23	579	21N-43N	75W-159W
Oct	25	716	21N-43N	75W-159W
Dec	10	326	21N-45N	72W-156W
Jan 1976	36	1119	9N-61N	180E-180W
Feb	54	1435	33S-43N	72W-114E
Mar	39	1057	9N-47N	180E-180W

Table 2. Number of ozone observations in  $10^{\circ}$  latitude intervals centered at the indicated latitudes for all longitudes (N< 15 is blank).

a. As a function of height for combined March, 1975, and March, 1976.

Height	Latitude				
	55°N	45	35	25	15
12-13 km			79	45	
11-12 km	47	198	140	144	95
10-11 km	187	231	233	127	35
9-10 km	139	152	71	67	
8 - 9 km	21	24	53		

b. As a function of time at 11-12 km.

[illegible]

Table 3. Mean, temporal standard deviation, and frequency distribution of GASP ozone data at 40-50°N. The mode is underlined at each level.

	Mean (ppbv)	St. Dev	No. Obs	No. Obs below Trop	Number of Obs. by Mixing Ratio				
					<100	<200	<300	<400	≥400ppbv
(a) Stratified by height									
<u>March 1975</u>									
11-12 km	302.4	165.2	58	11	10	4	12	12	<u>20</u>
10-11	360.3	235.2	100	30	28	3	7	7	<u>55</u>
9-10	173.4	158.8	95	84	<u>50</u>	14	9	5	<u>17</u>
8-9	149.4	<u>102.2</u>	15	14	<u>8</u>	1	4	2	0
	Av 171.9								
<u>March 1976</u>									
11-12 km	305.0	198.7	140	1	35	18	13	27	<u>47</u>
10-11	187.8	172.5	131	50	<u>67</u>	21	13	10	<u>20</u>
9-10	277.7	163.9	57	7	<u>11</u>	9	11	7	<u>19</u>
8-9	113.4	<u>123.7</u>	9	8	<u>6</u>	2	0	0	<u>1</u>
	Av 166.9								
<u>October 1975</u>									
12-13 km	75.3	50.1	44	29	<u>33</u>	10	1	0	0
11-12	64.4	50.4	106	81	<u>85</u>	16	5	0	0
10-11	30.9	<u>10.2</u>	14	13	<u>14</u>	0	0	0	0
	Av 41.4								
(b) Stratified by tropopause separation (hPa) ( $P_{Trop} - P_{Aircraft}$ )									
<u>March 1975</u>									
100 to 50 hPa	480.4	134.5	56		0	0	9	7	<u>40</u>
50 to 0	341.9	177.8	71		3	6	6	16	<u>40</u>
0 to - 50	149.8	122.2	108		<u>62</u>	16	17	3	<u>10</u>
-50 to -100	62.3	<u>44.2</u>	30		<u>30</u>	0	0	0	0
	129.0								
<u>March 1976</u>									
100 to 50 hPa	393.8	144.2	124		2	9	22	35	<u>56</u>
50 to 0	173.3	133.5	126		<u>58</u>	33	14	5	<u>16</u>
0 to - 50	73.6	39.5	58		<u>50</u>	6	2	0	0
-50 to -100	62.8	<u>24.0</u>	11		<u>10</u>	1	0	0	0
	100.9								
<u>October 1975</u>									
50 to 0 hPa	121.4	60.6	41		<u>18</u>	17	6	0	0
0 to - 50	53.3	27.7	58		<u>51</u>	7	0	0	0
-50 to -100	41.7	<u>22.0</u>	58		<u>55</u>	3	0	0	0
	40.5								



Table 4. Ozone mixing ratio, Trop-50 hPa to Trop+50 hPa, sorted according to the sign of  $w$ . Only data north of  $30^{\circ}\text{N}$  are used here. The number of observations is given in parentheses. The diffusive flux is based on  $K=3\times 10^3 \text{ cm}^2 \text{ s}^{-1}$ . See text.

	<u>Mean Ozone (ppbv)</u>		<u>Net Flux</u> (based on $\overline{ w } = 0.5 \text{ cm s}^{-1}$ )	<u>Diffusive</u> <u>Flux</u>
	Upward Motion	Downward Motion	( $10^{10} \text{ molec cm}^{-2} \text{ s}^{-1}$ )	( $10^{10} \text{ molec cm}^{-2} \text{ s}^{-1}$ )
Winter (D,J,F)	68.0 (887)	79.6 (907)	$9.0 \pm 2.5$	0.24
Spring (M,A,M)	214.7 (769)	227.3 (758)	$9.5 \pm 4.9$	0.25
Summer (J,J,A)	143.5 (126)	155.0 (126)	$7.9 \pm 8.2$	0.13
Autumn (S,O,N)	73.5 (231)	80.6 (151)	$4.7 \pm 3.3$	0.11
		Average	7.8	0.18

Table 5. North-south flux of ozone by transient eddies at  $40^{\circ}$ - $50^{\circ}$ N and 11-12 km with data divided into  $60^{\circ}$  longitude sets. The number of observations in each case is given in parentheses. Units are  $10^{-9} \text{ g cm}^{-2} \text{ s}^{-1}$ .

	<u><math>60^{\circ}\text{E}-0</math></u>	<u><math>0-60^{\circ}\text{W}</math></u>	<u><math>60-120^{\circ}\text{W}</math></u>	<u><math>120-180^{\circ}\text{W}</math></u>	<u><math>180-120^{\circ}\text{E}</math></u>
March 1975	-0.1 (2)	12.0 (8)	6.6 (21)	30.2 (27)	---
March 1976	-4.6 (9)	24.5 (29)	8.0 (54)	30.5 (30)	-48.4 (18)
Combined March	-7.8 (11)	28.1 (37)	8.2 (75)	40.1 (57)	-48.4 (18)

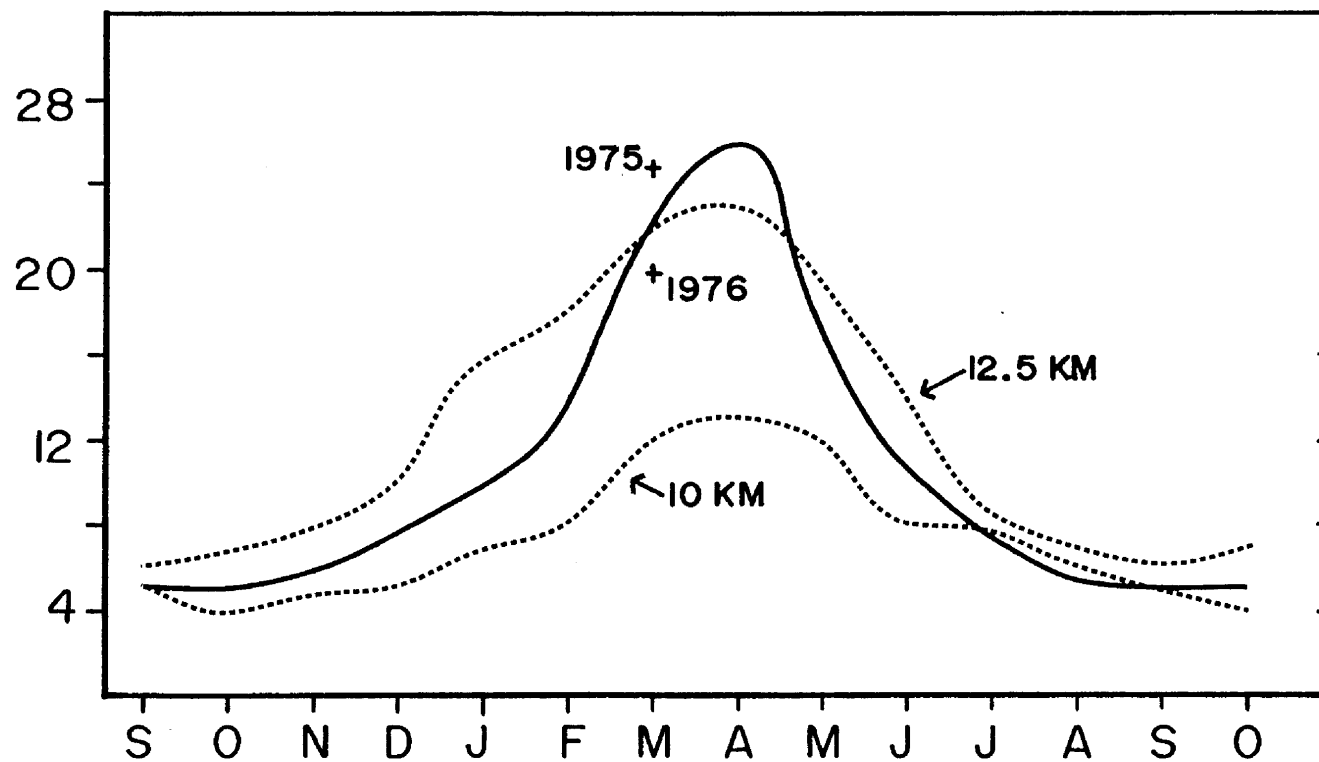


Figure 1. Heavy line is monthly mean variation of GASP ozone at 11-12 km, 36-42°N from March, 1975, through March, 1976. A 1-2-1 smoothing has been applied. Dotted lines are ozonesonde means at 40°N from Wilcox, et al (1975). Units:  $10^{11}$  molecules  $\text{cm}^{-3}$ .

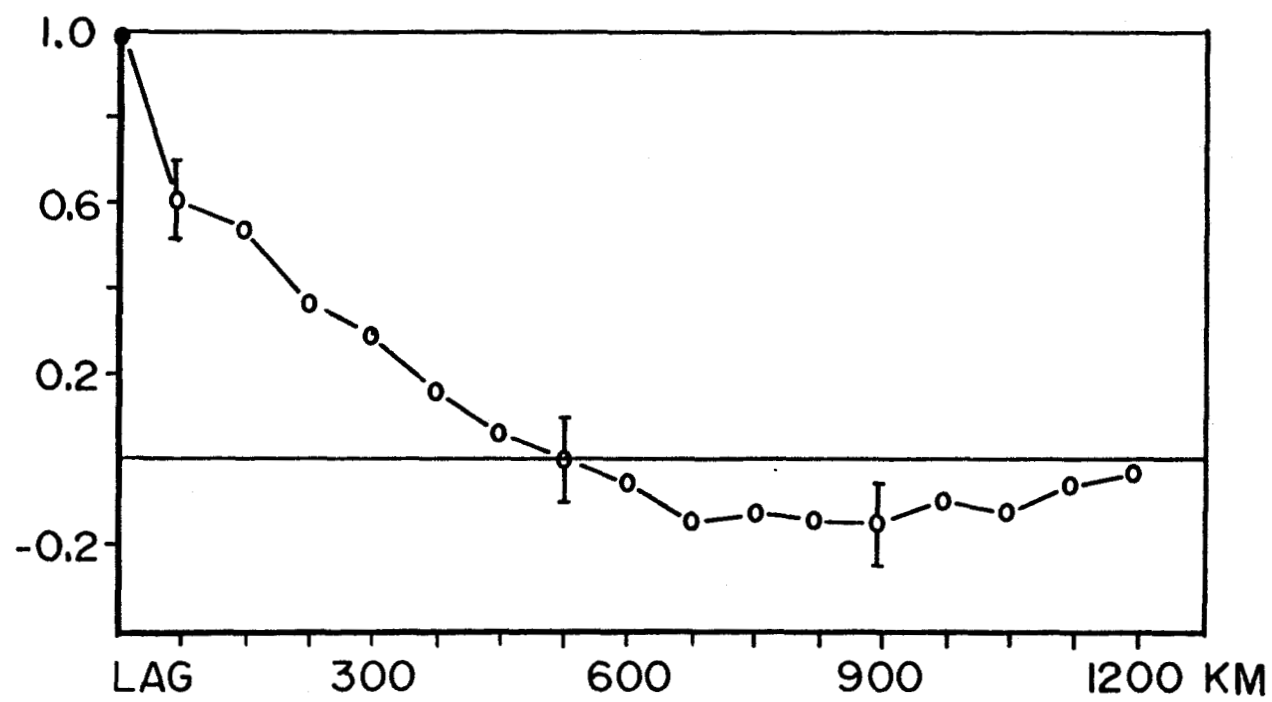


Figure 2. Distance lagged autocorrelation coefficients of ozone along east-west flight legs, based on 33 flights. See text.

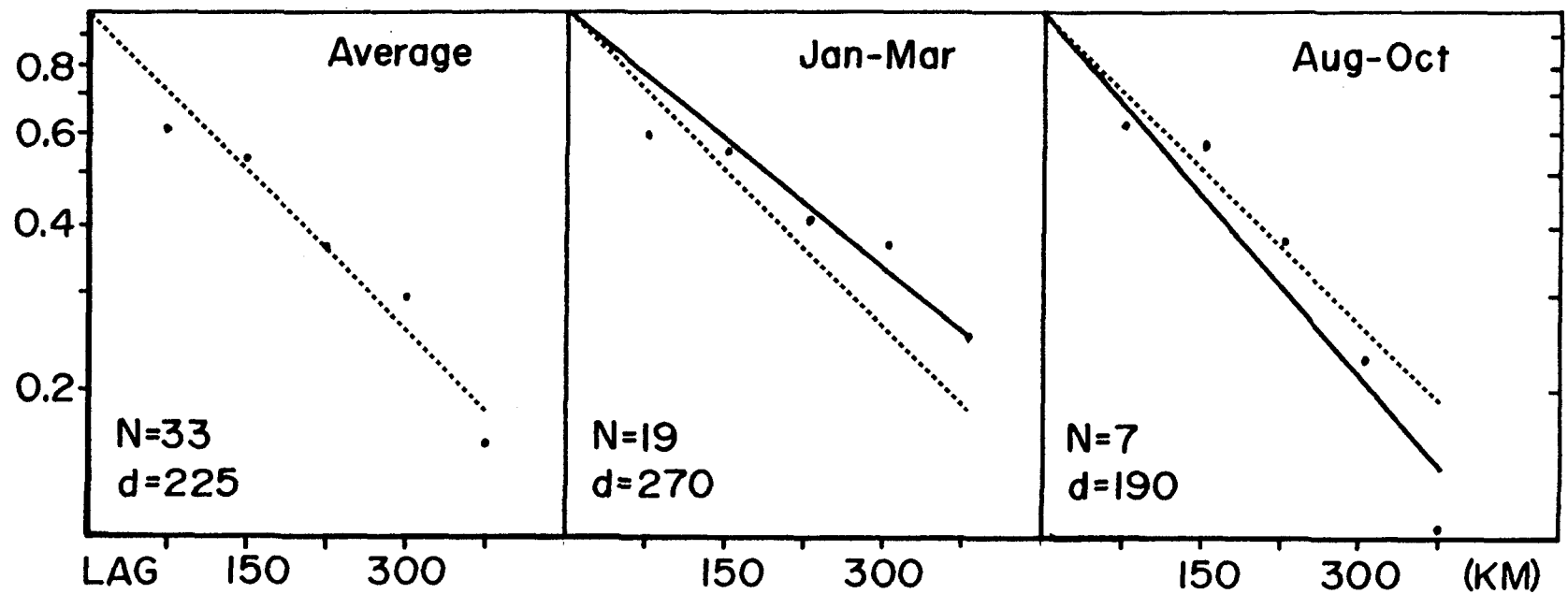


Figure 3. Distance lagged autocorrelation coefficients of ozone along east-west flight legs, for all data and by season. The dotted line on each chart is the least squares fit of  $R(L) = \exp(VL)$  to the "average" data and the solid lines are the fits to the seasonal data.  $N$  is the number of flights and  $d$  is the integral space scale of  $R(L)$ . See text.

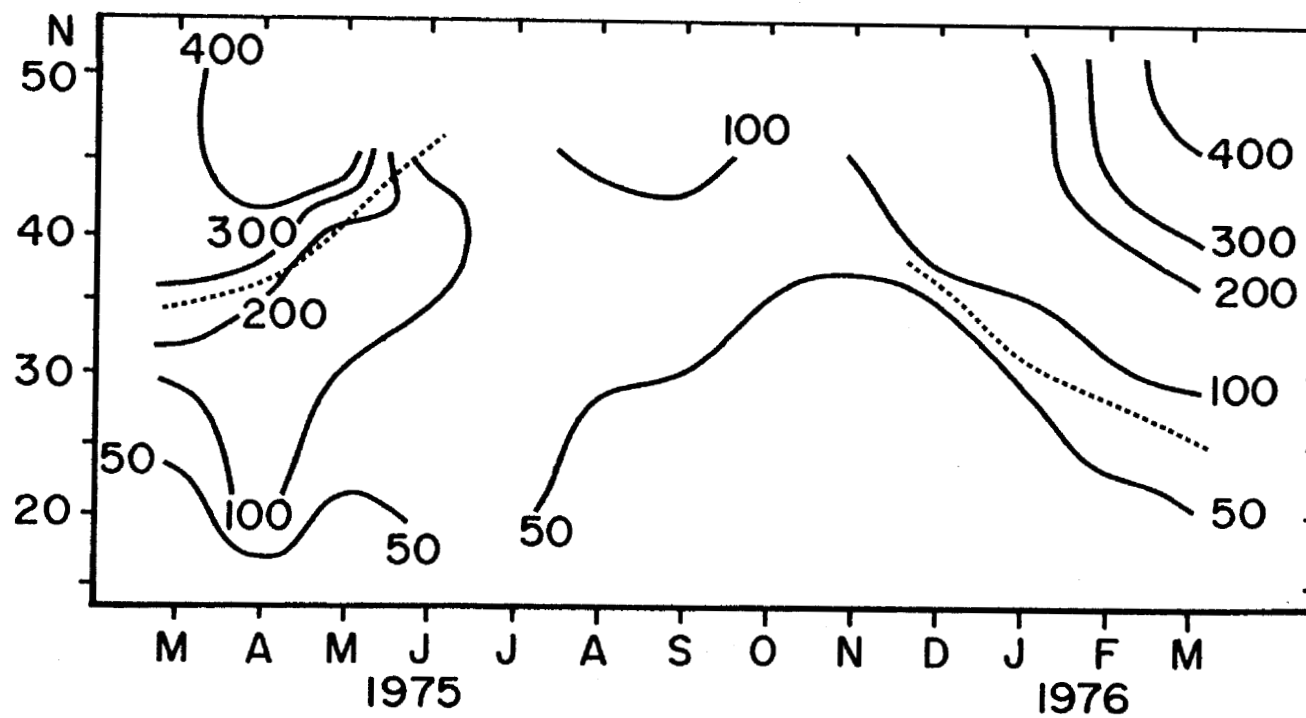


Figure 4. Monthly "zonal" means of ozone (ppbv) at 11-12 km. The dotted lines show the latitudes of the monthly mean tropopause at 11.5 km. Note that the Flattery tropopause model was used until December, 1975, and the Gustafson model thereafter.

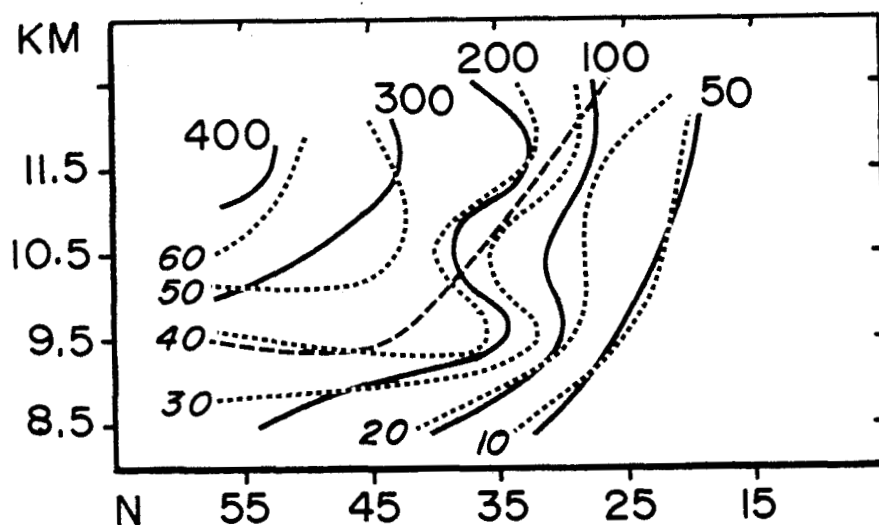


Figure 5. Solid lines are "zonal" means of ozone (ppbv) of  $10^\circ$  latitude belts for combined March data (1975 and 1976). The dashed line is mean tropopause location, and the dotted lines are "zonal" means of potential vorticity ( $10^{-6} \text{ deg hPa}^{-1} \text{ s}^{-1}$ ), for each belt.

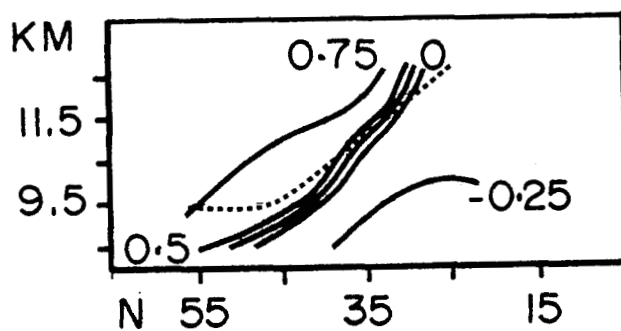


Figure 6. Correlation coefficients of ozone with temperature for combined March data (1975 and 1976). The dotted line is mean tropopause location.

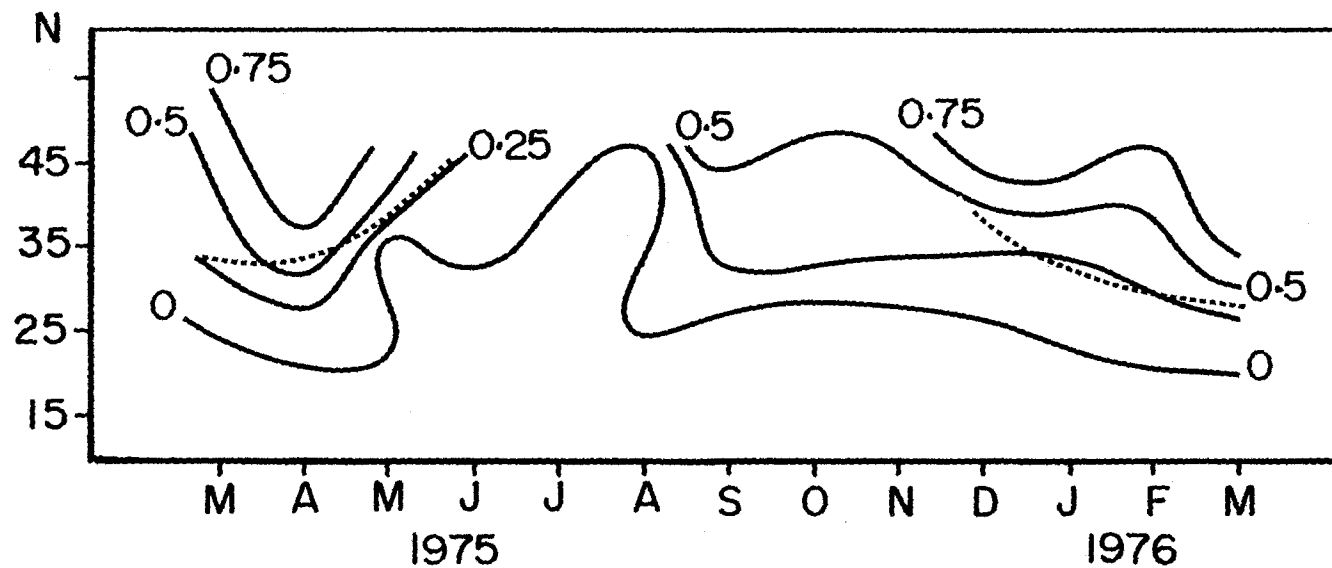


Figure 7. Correlation coefficients of ozone with temperature at 11-12 km by month. The dotted lines show the latitudes of the monthly mean tropopause at 11.5 km.



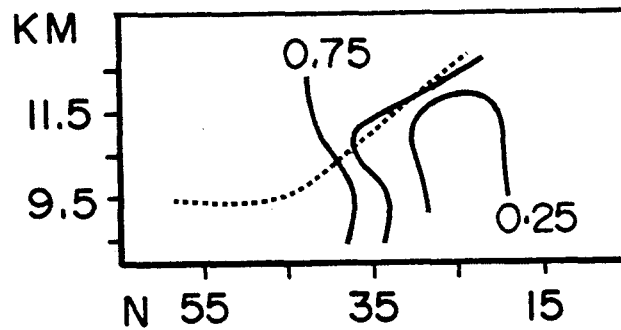


Figure 8. Correlation coefficients of ozone with potential vorticity for combined March data (1975 and 1976). The dotted line is mean tropopause location.

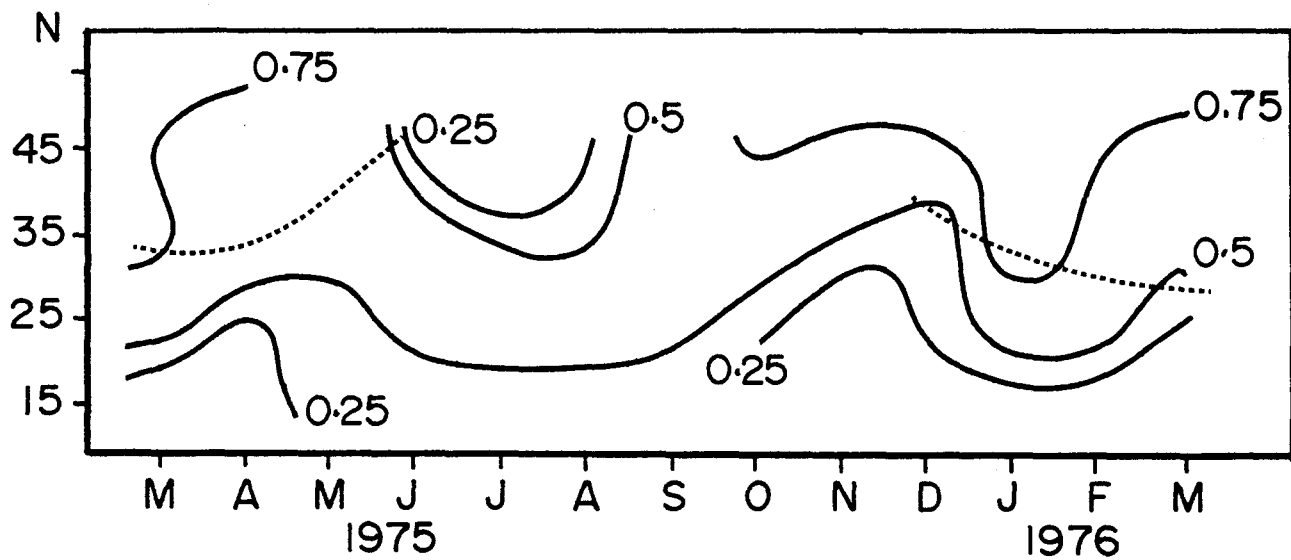


Figure 9. Correlation coefficients of ozone with potential vorticity at 11-12 km by month. The dotted lines show the latitudes of the monthly mean tropopause at 11.5 km.

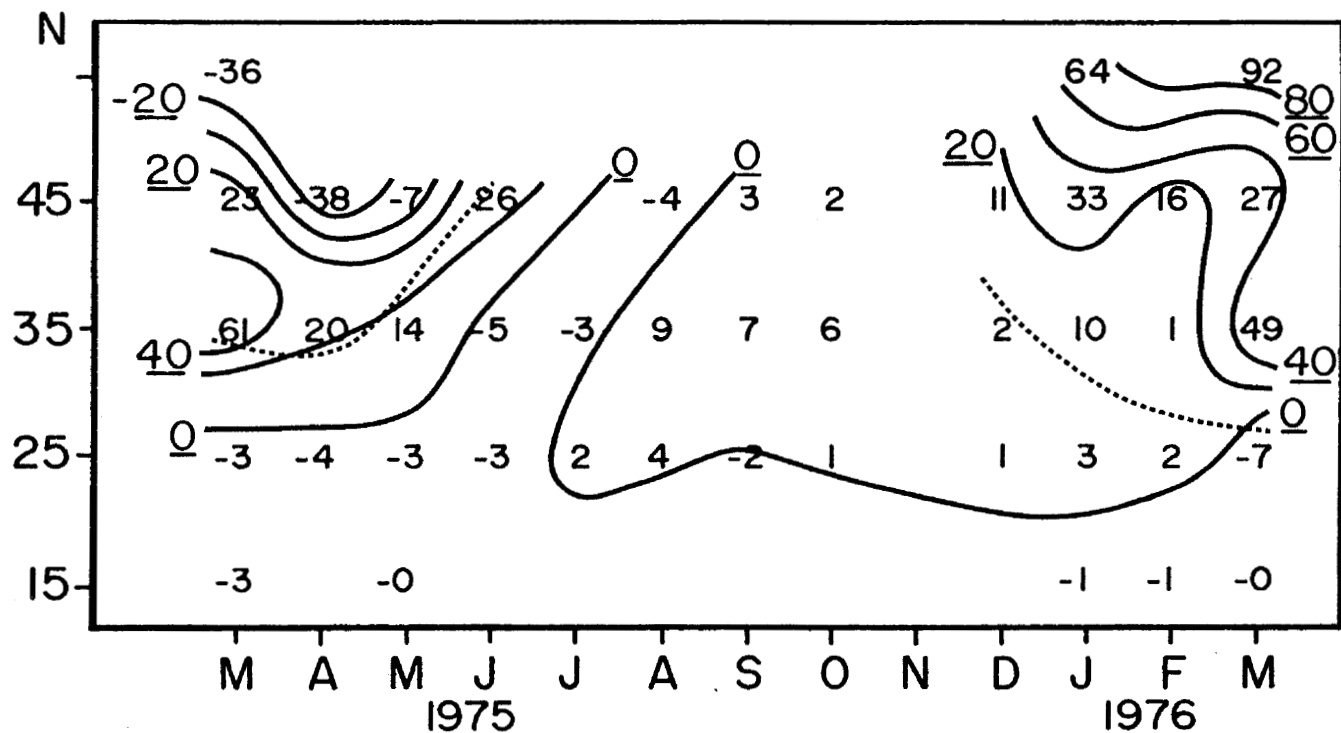


Figure 10. Northward flux of ozone by transient eddies at 11-12 km by month (units:  $10^{-9} \text{ g cm}^{-2} \text{ s}^{-1}$ ). The dotted lines show the latitudes of the monthly mean tropopause at 11.5 km. To avoid confusion, isoline labels are underlined.

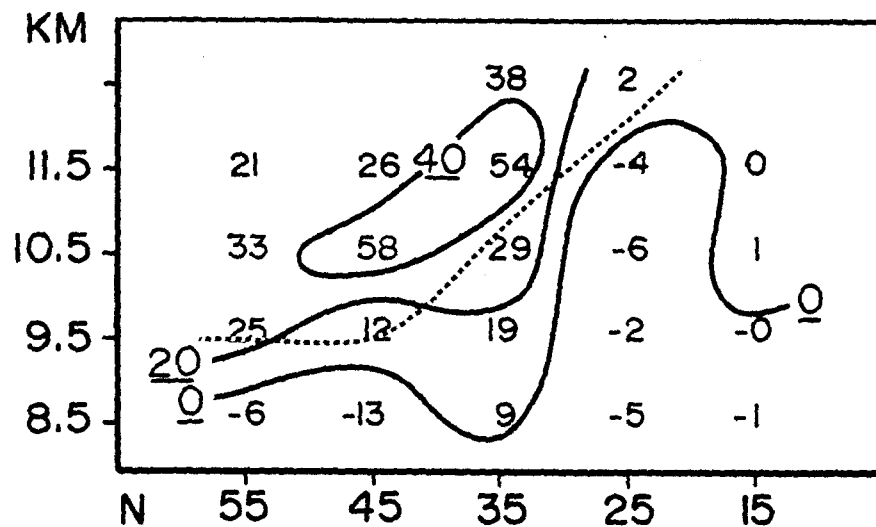


Figure 11. Northward flux of ozone by transient eddies for combined March data (1975 and 1976). Units:  $10^{-9} \text{ g cm}^{-2} \text{ s}^{-1}$ . The dotted line is mean tropopause location, and isoline labels have been underlined to avoid confusion.